Author/s:
Walia, S;Balendhran, S;Ahmed, T;Singh, M;El-Badawi, C;Brennan, MD;Weerathunge, P;Karim, MN;Rahman, F;Rassell, A;Duckworth, J;Ramanathan, R;Collis, GE;Lobo, CJ;Toth, M;Kotsakidis, JC;Weber, B;Fuhrer, M;Dominguez-Vera, JM;Spencer, MJS;Aharonovich, I;Sriram, S;Bhaskaran, M;Bansal, V

Title:
Ambient Protection of Few-Layer Black Phosphorus via Sequestration of Reactive Oxygen Species

Date:
2017-07-19

Citation:
Walia, S., Balendhran, S., Ahmed, T., Singh, M., El-Badawi, C., Brennan, M. D., Weerathunge, P., Karim, M. N., Rahman, F., Rassell, A., Duckworth, J., Ramanathan, R., Collis, G. E., Lobo, C. J., Toth, M., Kotsakidis, J. C., Weber, B., Fuhrer, M., Dominguez-Vera, J. M. ,... Bansal, V. (2017). Ambient Protection of Few-Layer Black Phosphorus via Sequestration of Reactive Oxygen Species. Advanced Materials, 29 (27), https://doi.org/10.1002/adma.201700152.

DOI: 10.1002/((please add manuscript number))
Article type: Communication

Ambient protection of few-layer black phosphorus via sequestration of reactive oxygen species

Sumeet Walia, Sivacarendran Balendhran, Taimur Ahmed, Mandeep Singh, Christopher El-Badawi, Mathew D. Brennan, Pabudi Weerathunge, Md. Nurul Karim, Fahmida Rahman, Andrea Rassell, Jonathan Duckworth, Rajesh Ramanathan, Gavin E. Collis, Charlene J. Lobo, Milos Toth, Jimmy Christopher Kotsakidis, Bent Weber, Michael Fuhrer, Jose Manuel Dominguez-Vera, Michelle J. S. Spencer, Igor Aharonovich, Sharath Sriram, Madhu Bhaskaran and Vipul Bansal**

Dr. S. Walia, Dr. S. Balendhran, Mr. T. Ahmed, Ms. F. Rahman, Assoc. Prof. S. Sriram, Assoc. Prof. M. Bhaskaran
Functional Materials and Microsystems Research Group and Micro Nano Research Facility, RMIT University, Melbourne VIC 3001, Australia
E-mail: sumeet.walia@rmit.edu.au

Mr. M. Singh, Ms. P. Weerathunge, Mr. Md. Nurul Karim, Dr. R. Ramanathan, Prof. V. Bansal
Ian Potter NanoBioSensing Facility, NanoBiotechnology Research Laboratory, School of Science, RMIT University, Melbourne 3000, Victoria, Australia
E-mail: vipul.bansal@rmit.edu.au

Mr. C. El-Badawi, Dr. C.J. Lobo, Prof. M. Toth, Assoc. Prof. I. Aharonovich
School of Mathematical and Physical Sciences, University of Technology Sydney, Ultimo 2007, NSW, Australia

Mr. M.D. Brennan, Assoc. Prof. M.J. Spencer
School of Science, RMIT University, Melbourne 3001, Victoria, Australia

Ms. A. Rassell, Dr. J. Duckworth
School of Media and Communication, RMIT University, Melbourne 3000, Victoria, Australia

Dr. G.E. Collis
CSIRO Manufacturing, CSIRO, Bayview Avenue, Clayton 3168, Victoria, Australia

Mr. J.C. Kotsakidis, Dr. B. Weber, Prof. M. Fuhrer
School of Physics and Monash Centre for Atomically Thin Materials, Monash University, Clayton 3800, Victoria, Australia

Prof. J.M. Dominguez-Vera

Departamento de Qu´ımica Inorganica, Facultad de Ciencias, Universidad de Granada, E-18071, Granada, Spain

ABSTRACT

Few-layer black phosphorous (BP) has emerged as a promising candidate for next generation nanophotonic and nanoelectronic devices. However, rapid ambient degradation of mechanically-exfoliated BP poses challenges in its practical deployment in scalable devices. To-date, the strategies employed to protect BP have relied upon preventing its exposure to atmospheric conditions. Here, we report an approach that allows this sensitive material to remain stable without requiring its isolation from the ambient environment. Our method draws inspiration from the unique ability of biological systems to avoid photo-oxidative damages caused by reactive oxygen species (ROS). Since BP undergoes similar photo-oxidative degradation, we employ imidazolium-based ionic liquids (ILs) as quenchers of these damaging species on the BP surface. This chemical sequestration strategy allows BP to remain stable for over thirteen weeks, while retaining its key electronic characteristics. This study opens opportunities to practically implement BP and other environmentally-sensitive two-dimensional (2D) materials for electronic applications.

Keywords: phosphorene, black phosphorus, two-dimensional materials, stability, ionic liquids, degradation

Few-layer black phosphorous (BP) has recently emerged as a promising candidate for next generation nanophotonic and nanoelectronic devices. The tunable intrinsic bandgap (~0.3 eV for bulk and ~2 eV for monolayer)[1,2], high carrier mobility and highly anisotropic properties of few-layer BP,[1,3-5] make it a desirable candidate for a variety of applications, including energy generation and storage systems as well as chemical/bio-sensing.[6-11] For most of these

applications, the material does not necessarily need to be in the form of a monolayer, but rather as a thin film, composite, or an embedded structure.[12]

A fundamental challenge hampering implementation of few-layer BP in practical scalable devices is its vulnerability to ambient degradation within a few hours.[13-15] As a result the material rapidly loses its semiconducting properties and is rendered unusable. The mechanism and causes of this degradation is still a subject of investigation, with recent reports indicating the combination of light and oxygen in the presence of ambient moisture being the key factor.[16,17] Considering that these factors play a synergistic role, analogies may be drawn between the BP degradation mechanism and biological systems. An elegant example is photosystem II chemistry in plants, wherein a combination of light and oxygen is known to produce highly oxidising radicals and reactive oxygen species (ROS) that are toxic to organisms.[18] However, the biological systems have the unique ability to protect and/or repair themselves from such photo-oxidative damages by employing a number of antioxidants.[18,19]

To-date, the strategies employed to protect BP have relied upon preventing its exposure to atmospheric conditions.[16,20] Chemical modifications have also been widely utilised to manipulate the optical and electronic properties of nanomaterials.[21-27] However, these approaches have not capitalised upon the antioxidant potential of molecules that could sequester the damaging ROS generated on the nanomaterial surface through environmental interactions, which eventually causes material degradation.

In this work, we carefully engineer a biomimetic platform to protect environmentally-sensitive 2D materials through their surface treatment with antioxidant molecules. Our method draws inspiration from the unique ability of biological systems to avoid photo-

oxidative damages caused by ROS.[19] Since BP undergoes similar photo-oxidative degradation,[10,16] we employ imidazolium-based ionic liquids (ILs) as quenchers of these damaging species on the BP surface. As such, we exploit the ROS quenching ability of ILs to stabilise few-layer BP against ambient oxidation. Our strategy fundamentally differs from the previously reported BP protection techniques, wherein the reported methods employ a blocking layer that acts as a physical barrier between the BP and the environment. This physical barrier may be in the form of a layer of inorganic material such as aluminium oxide, or a layer of organic molecules such as aryl diazonium ions that form covalent bonds with the free surface atoms of BP.[26,28-35] We acknowledge that the ability of ILs to act as appropriate exfoliation solvents to produce few-layer BP has been explored;[36] however the role of IL in actively sequestering ROS to protect BP against ambient degradation, thereby preserving its long-term electronic characteristics has not been considered. Therefore, an important distinction of our strategy is to employ ILs as a functional chemical barrier, which without strongly interacting with BP, actively participates in rapidly capturing any ROS that is generated on the BP surface via environmental interactions. This IL-mediated chemo-sequestration approach offers advantages in terms of (i) non-covalent modification of the BP surface, which may otherwise cause changes in the electronic properties of pristine BP, and (ii) an advance in protecting BP through directly targeting its mechanism of degradation under ambient conditions which eliminates the requirement of isolating the material from the environment, and therefore offering avenues to extending this new approach for the protection of other 2D materials that suffer from oxidative degradation. Additionally, ILs also have the potential for being employed as gate dielectrics to efficiently tune the Fermi energy in BP based electric-double-layer transistors.[37]

We choose two imidazolium based ILs, with the same 1-butyl-3-methylimidazolium [BMIM] cation, but with different anions. Tetrafluoroborate [BF_4] anion makes the IL highly polar, whereas hexafluorophosphate [PF_6] anion makes the IL non-polar. Our investigations begin with the hypothesis that the hydrophobicity of [BMIM][PF_6] may be more favourable in providing resistance against BP degradation, since ambient moisture is known to facilitate photo-oxidation of BP.[10,16] We treat the surface of 10-15 nm thick BP flakes (see supporting Figure S1) using these two ILs independently and test their effectiveness using an *in situ* environmental scanning electron microscopy (ESEM) technique.

ESEM is used to obtain insights into the oxidising chemical reactions that can degrade BP, and to monitor the degradation rate in real time (**Figure 1**). This is achieved by imaging BP using an electron beam whilst the ESEM vacuum chamber is filled with a small amount (~8 Pa) of H_2O vapour. Electron irradiation under such conditions is known to generate highly reactive radicals similar to ROS that give rise to oxidation in the vicinity of the electron beam, thereby leading to chemical etching of even inert materials such as diamond.[38] Figure 1a shows a schematic representation of this process. Here, the radicals give rise to the rapid degradation of pristine BP within 15 min of imaging (corresponding to an electron irradiation fluence of 2.71×10^{19} electrons·cm^{-2}) as seen in Figure 1b and Supporting Video 1. The evolution of pristine BP surface degradation is further captured using time-lapse AFM imaging (Supporting Videos 2 and 3)

In contrast, the IL-treated samples are significantly more resilient and able to withstand more aggressive electron exposures. The [BMIM][PF_6]-treated BP deteriorates only partially after 120 min of electron exposure (corresponding to an electron fluence of 5.43×10^{21} electrons per square cm), as is seen in Figure 1c and Supporting Video 4. The [BMIM][BF_4]-treated BP is highly stable and resilient even after 180 min of exposure and a total electron beam fluence of

1.58×10^{22} electrons per square cm (see Figure 1d and Supporting Video 5). To confirm that the BP degradation seen in the ESEM images is caused by oxidising radicals generated through the dissociation of H_2O rather than by direct electron beam damage, reference exposures were performed in high vacuum (~3×10^{-4} Pa), where the observed degradation rate is several orders of magnitude lower than in the presence of 8 Pa of H_2O vapour (see Figure S2 in the Supporting Information). Hence, our *in situ* ESEM studies validate the dominant role of ROS in BP degradation, while establishing that the relative hydrophobicity of [BMIM][PF_6] (shown in Figure 1c) does not result in superior stabilisation of BP.

To obtain insights into the nature of binding of ILs to BP, we performed density functional theory (DFT) calculations (**Figure 2**). The modelling studies for both basal and edge planes of BP reveal the chemisorption of [BMIM] cation without forming a covalent bond, such that the association of the IL ion-pairs to BP is slightly stronger in case of [BMIM][BF_4] over [BMIM][PF_6] (other optimised structures are shown in Supporting Information, Figures S3-S8). As BP degradation is observed to initiate from its edge plane, we also modelled the influence of the crowding effect of ILs at the BP edge. Introduction of an additional molecule makes IL binding to BP more favourable without influencing their relative binding affinity towards BP. Even though in the case of both ILs, the chemisorption of [BMIM] cation to BP through its imidazole ring is thermodynamically favoured; the electrostatic interactions between the anion and the cation play an important role in dictating the overall binding energies of the two ILs. Further, the binding of the ILs to BP appears to cause minor lattice distortions, similar to those observed previously, when aryl diazonium chemistry was explored for surface passivation of exfoliated BP.[26] It may be noted that our DFT studies have focussed on a single phosphorene monolayer, largely due to the requirement of significantly longer computation time for multilayer BP, along with the established fact that

the binding energy between multiple phosphorene layers is known to be dominated by van der Waals type forces.[39] Therefore, we would expect that adsorbing the ILs on a multi-layer phosphorene structure is unlikely to have a significant effect on the interaction energy. This is further supported by our DFT studies which reveal that the positions of the individual P atoms in the phosphorene monolayer are little changed after the IL adsorption. This indicates that the IL-BP interactions are localised to the outermost, and closest, P atoms. Hence, we would expect that adding layers of P to the model will not significantly change the results and influence the conclusions that we draw. As such, theoretical and experimental studies collectively reveal that stronger binding of [BMIM][BF_4] to BP makes it a superior stabilising agent compared to [BMIM][PF_6]. It is also noted that ILs with [PF_6] anions are not very stable under ambient conditions and may gradually produce corrosive species, such as HF, which may be responsible for partial degradation of BP flakes observed under ESEM.[40] As a result, we further focus our investigations on studying the role of [BMIM][BF_4] IL in BP stabilisation and its use in practical devices.

We employ X-ray photoelectron spectroscopy (XPS) to study the binding of [BMIM][BF_4] to the BP surface and its effect on stabilisation (**Figure 3**a and Supporting Figure S9). The chemical nature of surface-treated BP was probed with C 1*s*, N 1*s*, P 2*p*, B 1*s* and F 1*s* core level XPS spectra, background corrected using Shirley algorithm, and deconvoluted into individual components using a Gaussian-Lorentzian function. The P 2*p* core level binding energies show features corresponding to P-P (130 eV), P-C (132.5 eV), P-N (133.5 eV) and P-O (134.1 eV), which agree well with literature assignments (Figure 3a).[26,31] The P-C (284 eV)[26] and P-N (401.1 eV) signatures are also observed in the C 1*s* and N 1*s* spectra, supporting the chemisorption of the imidazolium ring observed in DFT modelling. Additional signatures corresponding to B 1*s* and F 1*s* core levels reflect the presence of [BF_4] anion,

through the [BMIM][BF_4] IL chemisorbed on the BP surface, as also observed through DFT studies. The relative stability of IL-treated BP over pristine BP is also evident from XPS, which shows that while the pristine BP readily oxidises within 72 h, the surface-treated BP remains largely stable. A marked decrease in the intensity of P–O feature in surface-treated BP confirms the ability of [BMIM][BF_4] in protecting BP against ambient degradation.

We next utilise confocal Raman spectroscopy to evaluate the ambient stability of the pristine and [BMIM][BF_4]-treated BP flakes (Figure 3b). BP exhibits three distinct Raman modes at 361 cm^{-1} (A^1_g mode), 438 cm^{-1} (B^2_g mode) and 465 cm^{-1} (A^2_g mode). The A^1_g mode originates primarily from the out-of-plane vibrations of phosphorus atoms along the *c*-axis, while the B^2_g and A^2_g modes arise from the in-plane vibrations of phosphorus atoms along the *b*-axis (armchair) and *a*-axis (zigzag), respectively.[41] The A^1_g mode is considered for the mapping as it remains constant when normalized to the Si transverse optical mode and hence provides a good reference for comparison.[42] In case of the pristine BP, the intensity of the A^1_g mode becomes non-existent within a week. However, the [BMIM][BF_4]-treated sample shows a largely non-variant intensity map even after 36 days of ambient storage and multiple cycles of exposure to a Raman laser. To quantify these observations, average peak intensities (normalised to the respective day 1 values) acquired on multiple flakes from each of the samples are analysed (Figure 3c). All three Raman modes show almost complete decay by Day 08 in the case of pristine BP (see Supporting Information Figure S10 for the corresponding pixel-by-pixel raw map and an analysis of the B^2_g and A^2_g modes). In contrast, the intensity average for the [BMIM][BF_4]-treated BP flakes, remains largely consistent, showing an intensity drop in the range of 7.5–9.0% over a period of 36 days. We attribute this drop to the laser induced photo-oxidation of BP during multiple cycles of Raman spectral mapping. In fact, to circumvent this issue, researchers typically deposit an aluminium oxide

passivating layer on BP flakes prior to extended Raman measurments, which is not required in our case. The average trend observed in multiple BP crystallites coupled with the spatial Raman analysis further highlights the effectivness of the proposed [BMIM][BF_4] IL-based surface treatment methodology against ambient degradation of BP. The potential of [BMIM][BF_4] IL in protecting BP flakes is further supported by AFM time-lapse videos on pristine (Supporting Videos 2 and 3) and IL-treated BP flakes (Supporting Video 6). We also located sub-10 nm flakes to verify the effectiveness of the IL-treatment on thinner flakes by employing Raman mapping over a period of 15 days (see Supporting Information Figure S11). We chose two flakes of thicknesses ca. 6 nm and 9 nm respectively, which along with original data on ca. 10-15 nm flakes, allows a comparison of the effectiveness of IL protection on BP flakes of different thicknesses. The 6 nm flake was chosen from a sample exfoliated and IL-treated under ambient, whereas the 9 nm flake was exfoliated and IL-treated under inert N_2 environment. As thinner flakes are more prone to ambient degradation, this choice allows us to validate the rigour of IL protection on thinner flakes produced under ambient conditions as well. During this period, we did not observe any noticeable influence on the ability of IL to protect BP flakes obtained under different exfoliation conditions, viz. inert vs. ambient. In general, pristine BP flakes degrade completely in less than a week (Figure 3b). As such, even though BP might get slightly oxidized when exfoliated under ambient conditions; those minor oxidation events do not interfere with the protective ability of ILs against further ambient oxidation as indicated by the comparison between the stability of two samples as shown in Supporting Information Figure S11. Next we focus on understanding the mechanism responsible for protective effects of [BMIM][BF_4] IL. Exposure of BP to light and molecular oxygen leads to ROS generation,[43] which are considered to play a dominant role in BP degradation,[16] as also experimentally validated through our current ESEM studies (Figure 1). Analogously, in biological systems, natural

antioxidants, such as carotenoids, play an important role in neutralising such damaging ROS.[19] Artificial compounds such as imidazoles have also been found to sequester these damaging species.[44] As such, to understand the underlying role of [BF_4]-based imidazolium IL in BP protection, we performed biochemical assays that assess the IL-mediated quenching of three different ROS, namely, singlet oxygen species ($^1O_2$), as well as hydroxyl ($OH^{\cdot}$) and superoxide ($O_2^{\cdot -}$) radicals (**Figure 4**) (see Supporting Information Section 7 for details). A schematic representation of the mechanism is provided in Figure 4a, illustrating that photogenerated ROS becomes non-accessible to the BP surface owing to the IL-facilitated sequestration. It is seen from Figure 4b that when photogenerated $^1O_2$ is exposed to as low as femtomolar concentrations of [BMIM][BF_4], this IL can sequester and quench ~90% of this damaging species. Other free radical species ($OH^{\cdot}$ and $O_2^{\cdot -}$) are also quenched to the similar levels, albeit requiring millimolar concentrations of IL. Therefore, it is inferred that [BMIM][BF_4] provides a unique ability to protect BP *via* sequestration of the damaging ROS.

To elucidate the applicability of our method to real world devices, we fabricate a field effect transistor (FET) from the [BMIM][BF_4]-treated BP. **Figure 5**a shows the *I–V* curves of a surface-treated BP FET at varying gate voltages. Figure 5b and 5c show a comparison of the transfer characteristics (I_D *vs* V_G) and transconductance obtained from a FET on a pristine and a [BMIM][BF_4]-treated BP flake, respectively. It is seen that the performance of the pristine sample deteriorates rapidly within 8 days resulting in a total loss of switching properties. On the other hand, treatment with [BMIM][BF_4] preserves the electrical characteristics for 92 days.

In summary, we demonstrate a robust procedure to stabilise mechanically-exfoliated few-layer black phosphorus (BP) and protect it from oxidation and deterioration. This makes BP amenable to device engineering. In particular, we first affirm the damaging role of reactive

oxygen species using an *in situ* ESEM study. Subsequently, we show that [BMIM][BF_4] ionic liquid can effectively sequester these reactive oxygen species, thereby preventing photo-oxidative degradation of BP flakes under ambient conditions. The chemical mechanism of the ionic liquid chemisorption to the BP flakes is studied using DFT modelling. The surface-treated BP retains its key electronic characteristics for 92 days. This chemical sequestration strategy offers new post-synthesis possibilities of employing chemical species with antioxidant properties to protect environmentally-sensitive 2D materials against photo-oxidative damages. In addition, since ILs offer potential as a solvent for liquid phase exfoliation synthesis of 2D materials,[36] mechanistic findings from this study will assist in improving the efficiency of current liquid phase exfoliation strategies. Further investigations into this technique have the potential of achieving tunability of electronic/optoelectronic as well as chemical properties of BP, enabling functional 2D materials and systems.

Experimental Section

Synthesis and treatment: For all the experiments conducted in this work, few-layer BP crystals were obtained *via* poly-dimethyl-siloxane (PDMS) assisted micromechanical exfoliation of commercial bulk black phosphorus crystals (Smart Elements) on a 50 nm SiO_2/Si substrate that were pre-cleaned using acetone and isopropanol and dried with high purity, compressed N_2. Surface treatment was carried out straight after the synthesis process by drop-casting the ILs on two separate samples. The ILs were left on the surface for ~40 min before being intensively washed off using acetonitrile and blow dried with N_2.

In situ ESEM: Electron beam irradiation was performed on pristine mechanically exfoliated few-layered BP on a SiO_2/Si substrate as well as IL-treated BP flakes. The samples were loaded in a variable pressure NanoSEM field emission gun SEM. The system was pumped

down to a base pressure of 3×10^{-4} Pa. Water vapour was then injected into the chamber so as to achieve a chamber pressure of 8 Pa. The BP flakes were imaged using a magnetic-field-assisted gaseous secondary electron detector. Electron beam irradiation was performed by imaging the samples repeatedly with a 20 keV, 1.35 nA electron beam using a scan rate of 3.36 ms/line and 1452 lines/frame. The flakes were exposed for up to three hours, as indicated in the figures.

Raman spectroscopy: The spatial Raman peak intensity mapping was conducted on a Horiba LabRAM Evolution micro-Raman system equipped with 9 mW, 532 nm laser (0.5 μm lateral resolution, 0.25 s exposure), and a 50× objective.

AFM: AFM imaging was conducted on a Dimension Icon AFM in Scan Assist mode.

ROS quenching studies: The ability of [BMIM][BF_4] IL to quench ROS was performed by assessing its impact on independently sequestering three oxidative species, namely $^1O_2$, O_2^- and $^{\cdot}OH$. These respective species were produced through photo-excitation of methylene blue, hypoxanthine/xanthine oxidase, and horseradish peroxidase, as elaborated in the Supporting Information Section 7.

BP FET fabrication and characterisation: FETs were fabricated on mechanically-exfoliated BP on 50 nm SiO_2/Si substrates. After the transfer, a photoresist layer was spin-coated at 4,000 rpm for 45 s followed by 100 ºC soft bake. The electrode patterns were UV-exposed using a mask aligner system (MA6, SUSS MicroTech) and subsequently developed. The metal electrodes Cr/Au (10/100 nm) were then deposited on the developed patterns using electron beam evaporation. Finally, the lift-off in acetone was carried out to reveal the required metallic contact pads for micro-probes and electrical measurement. The FET measurements were conducted using a Keithley 4200SCS semiconductor parameter analyser.

All measurements were performed under ambient conditions. The electrical characteristics were measured weekly for 36 days in parallel with the Raman measurements. Beyond that, the sample was left under ambient conditions and retested after 92 days.

Supporting Information

Supporting Information is available from the Wiley Online Library or from the authors

Acknowledgements
S.W. and S.B. contributed equally. The authors acknowledge the Australian Research Council for funding in the form of fellowship (DE150100909, DE160100023, DE160101334 and FT140101285), project (DP130100062 and DP140100170) and infrastructure (LE0882246, LE0989615, and LE150100001) support. The facilities and technical assistance of the Micro Nano Research Facility (MNRF) and the RMIT Microscopy and Microanalysis Research Facility (RMMF) are acknowledged. The computations were undertaken with the assistance of resources from the National Computational Infrastructure (NCI), which is supported by the Australian Government, the Pawsey Supercomputing Centre with funding from the Australian Government and the Government of Western Australia, and the Multimodal Australian ScienceS Imaging and Visualisation Environment (MASSIVE).

Received: ((will be filled in by the editorial staff))
Revised: ((will be filled in by the editorial staff))
Published online: ((will be filled in by the editorial staff))

References

[1] V. Tran, R. Soklaski, Y. Liang, L. Yang, *Phys. Rev. B.* 2014, **89**, 235319.
[2] S. Das, W. Zhang, M. Demarteau, A. Hoffmann, M. Dubey, A. Roelofs, *Nano Lett.* 2014, **14**, 5733.
[3] M. Buscema, D. J. Groenendijk, S. I. Blanter, G. A. Steele, H. S. van der Zant, A. Castellanos-Gomez, *Nano Lett.* 2014, **14**, 3347.
[4] H. Liu, A. T. Neal, Z. Zhu, Z. Luo, X. Xu, D. Tománek, P. D. Ye, *ACS Nano* 2014, **8**, 4033.
[5] F. Xia, H. Wang, Y. Jia, *Nat. Commun.* 2014, **5**, 4458.
[6] Y. Chen, R. Ren, H. Pu, J. Chang, S. Mao, J. Chen, *Biosens. Bioelectron.* 2016, **89**, 505.
[7] J. Dai, X. C. Zeng, *J. Phys. Chem. Lett.* 2014, **5**, 1289.
[8] W. Li, Y. Yang, G. Zhang, Y.-W. Zhang, *Nano Lett.* 2015, **15**, 1691.
[9] M. Z. Rahman, C. W. Kwong, K. Davey, S. Z. Qiao, *Energ. Environ. Sci.* 2016, **9**, 709.

[10] D. Hanlon, C. Backes, E. Doherty, C. S. Cucinotta, N. C. Berner, C. Boland, K. Lee, A. Harvey, P. Lynch, Z. Gholamvand, *Nat. Commun.* 2015, **6**, 8563.
[11] S. Balendhran, S. Walia, H. Nili, S. Sriram, M. Bhaskaran, *Small* 2015, **11**, 640.
[12] P. Yasaei, A. Behranginia, T. Foroozan, M. Asadi, K. Kim, F. Khalili-Araghi, A. Salehi-Khojin, *ACS Nano* 2015, **9**, 9898.
[13] J. O. Island, G. A. Steele, H. S. van der Zant, A. Castellanos-Gomez, *2D Mater.* 2015, **2**, 011002.
[14] J.-S. Kim, Y. Liu, W. Zhu, S. Kim, D. Wu, L. Tao, A. Dodabalapur, K. Lai, D. Akinwande, *Sci. Rep.* 2015, **5**, 8989.
[15] L. Kou, C. Chen, S. C. Smith, *J. Phys. Chem. Lett.* 2015, **6**, 2794.
[16] A. Favron, E. Gaufrès, F. Fossard, A.-L. Phaneuf-L'Heureux, N. Y. Tang, P. L. Lévesque, A. Loiseau, R. Leonelli, S. Francoeur, R. Martel, *Nat. Mater.* 2015, **14**, 826.
[17] S. Walia, Y. Sabri, T. Ahmed, M. R. Field, R. Ramanathan, A. Arash, S. K. Bhargava , S. Sriram, M. Bhaskaran, V. Bansal, S. Balendhran, *2D Mater.* 2017, **4**, 015025.
[18] J. Barber, B. Andersson, *Trends Biochem. Sci.* 1992, **17**, 61.
[19] F. Böhm, R. Edge, T. George Truscott, *Acta Biochim. Pol.* 2012, **59**, 27.
[20] J. D. Wood, S. A. Wells, D. Jariwala, K.-S. Chen, E. Cho, V. K. Sangwan, X. Liu, L. J. Lauhon, T. J. Marks, M. C. Hersam, *Nano Lett.* 2014, **14**, 6964.
[21] C. Xie, X. Zhang, Y. Wu, X. Zhang, X. Zhang, Y. Wang, W. Zhang, P. Gao, Y. Han, J. Jie, *J. Mater. Chem. A* 2013, **1**, 8567.
[22] A. G. Aberle, *Prog. Photovolt: Res. Appl.* 2000, **8**, 473.
[23] J. Shen, Y. Zhu, X. Yang, J. Zong, J. Zhang, C. Li, *New J. Chem.* 2012, **36**, 97.
[24] J. Wang, *Electroanal.* 2005, **17**, 7.
[25] J. Zhang, X. Liu, R. Blume, A. Zhang, R. Schlögl, D. S. Su, *Science* 2008, **322**, 73.
[26] C. R. Ryder, J. D. Wood, S. A. Wells, Y. Yang, D. Jariwala, T. J. Marks, G. C. Schatz, M. C. Hersam, *Nat. Chem.* 2016, **8**, 597.
[27] Y. Zhao, H. Wang, H. Huang, Q. Xiao, Y. Xu, Z. Guo, H. Xie, J. Shao, Z. Sun, W. Han, *Angew. Chem.* 2016, **128**, 5087.
[28] G. Abellán, V. Lloret, U. Mundloch, M. Marcia, C. Neiss, A. Görling, M. Varela, F. Hauke, A. Hirsch, *Angew. Chem.* 2016, **128**, 14777.
[29] A. Avsar, I. J. Vera-Marun, J. Y. Tan, K. Watanabe, T. Taniguchi, A. H. Castro Neto, B. Ozyilmaz, *ACS Nano* 2015, **9**, 4138.
[30] R. A. Doganov, E. C. O'Farrell, S. P. Koenig, Y. Yeo, A. Ziletti, A. Carvalho, D. K. Campbell, D. F. Coker, K. Watanabe, T. Taniguchi, *Nat. Commun.* 2015, **6**.
[31] M. Edmonds, A. Tadich, A. Carvalho, A. Ziletti, K. O'Donnell, S. Koenig, D. Coker, B. Özyilmaz, A. C. Neto, M. Fuhrer, *ACS Appl. Mater. Int.* 2015, **7**, 14557.
[32] J. Kang, J. D. Wood, S. A. Wells, J.-H. Lee, X. Liu, K.-S. Chen, M. C. Hersam, *ACS Nano* 2015, **9**, 3596.
[33] H. Liu, A. T. Neal, M. Si, Y. Du, D. Y. Peide, *IEEE Electron Device Letters* 2014, **35**, 795.
[34] J. Pei, X. Gai, J. Yang, X. Wang, Z. Yu, D.-Y. Choi, B. Luther-Davies, Y. Lu, *Nat. Commun.* 2016, **7**.
[35] A. H. Woomer, T. W. Farnsworth, J. Hu, R. A. Wells, C. L. Donley, S. C. Warren, *ACS Nano* 2015, **9**, 8869.
[36] W. Zhao, Z. Xue, J. Wang, J. Jiang, X. Zhao, T. Mu, *ACS Appl. Mater. Int.* 2015, **7**, 27608.
[37] Y. Saito, Y. Iwasa, *ACS Nano* 2015, **9**, 3192.
[38] A. A. Martin, A. Bahm, J. Bishop, I. Aharonovich, M. Toth, *Phys. Rev. Lett.* 2015, **115**, 255501.

[39] L. Shulenburger, A. D. Baczewski, Z. Zhu, J. Guan, D. Tomanek, *Nano Lett.* 2015, **15**, 8170.
[40] R. P. Swatloski, J. D. Holbrey, R. D. Rogers, *Green Chem.* 2003, **5**, 361.
[41] A. Łapińska, A. Taube, J. Judek, M. Zdrojek, *J. Phys. Chem. C.* 2016, **120**, 5265.
[42] S. Zhang, J. Yang, R. Xu, F. Wang, W. Li, M. Ghufran, Y.-W. Zhang, Z. Yu, G. Zhang, Q. Qin, *ACS Nano* 2014, **8**, 9590.
[43] H. Wang, X. Yang, W. Shao, S. Chen, J. Xie, X. Zhang, J. Wang, Y. Xie, *J. Am. Chem. Soc.* 2015, **137**, 11376.
[44] L. Zhao, C. Zhang, L. Zhuo, Y. Zhang, J. Y. Ying, *J. Am. Chem. Soc.* 2008, **130**, 12586.

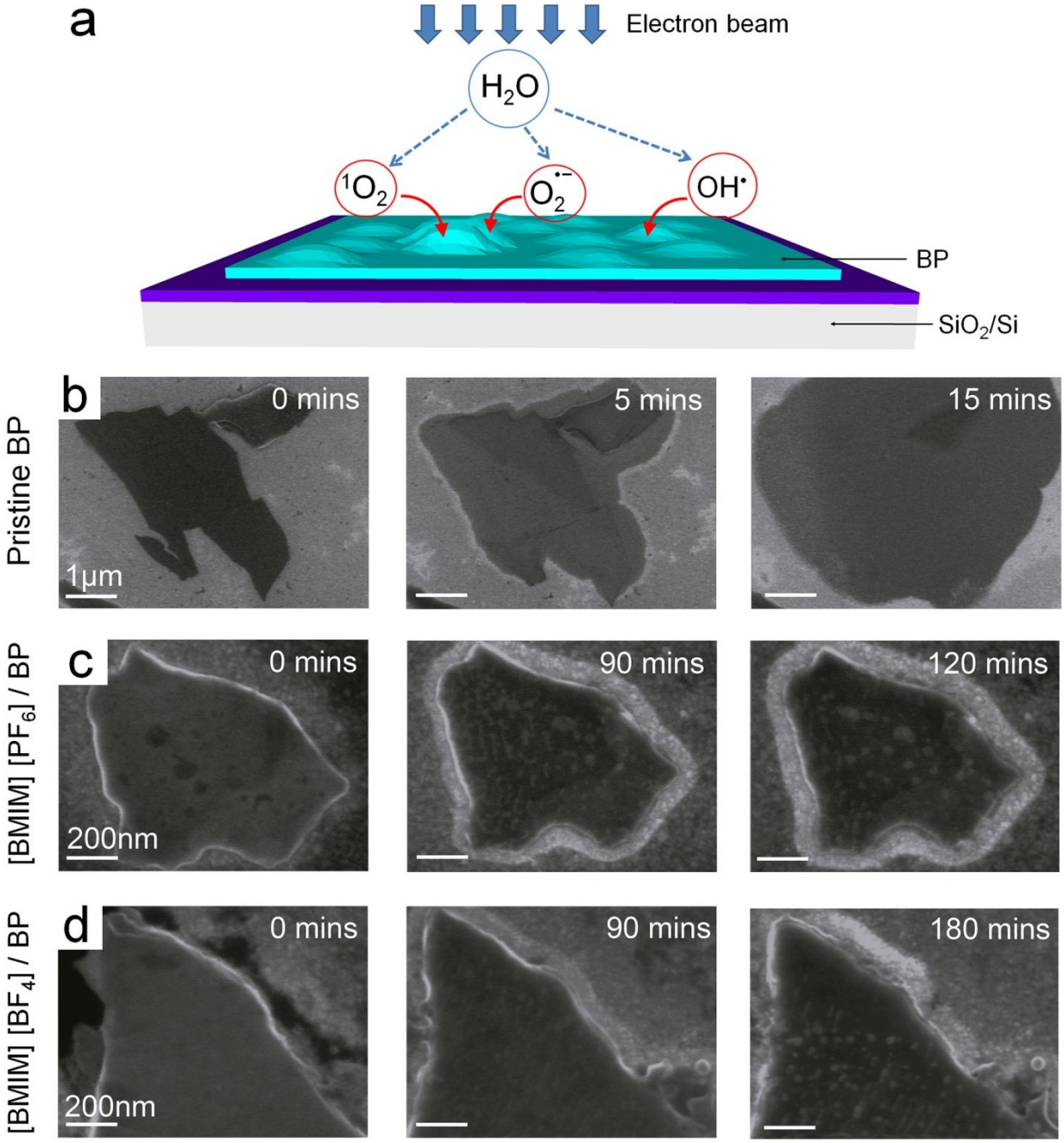

Figure 1. a) Schematic representation of the electron beam induced ROS production that causes degradation of an unprotected BP surface. b-d) ESEM micrographs of the BP flakes imaged in the presence of H_2O vapour. b) pristine BP. c) [BMIM][PF_6]-treated BP and d) [BMIM][BF_4]-treated BP flakes. The flake in **b** deteriorated and shrunk rapidly into the small dark feature as seen in the figure, as well as in Supporting Video 1.

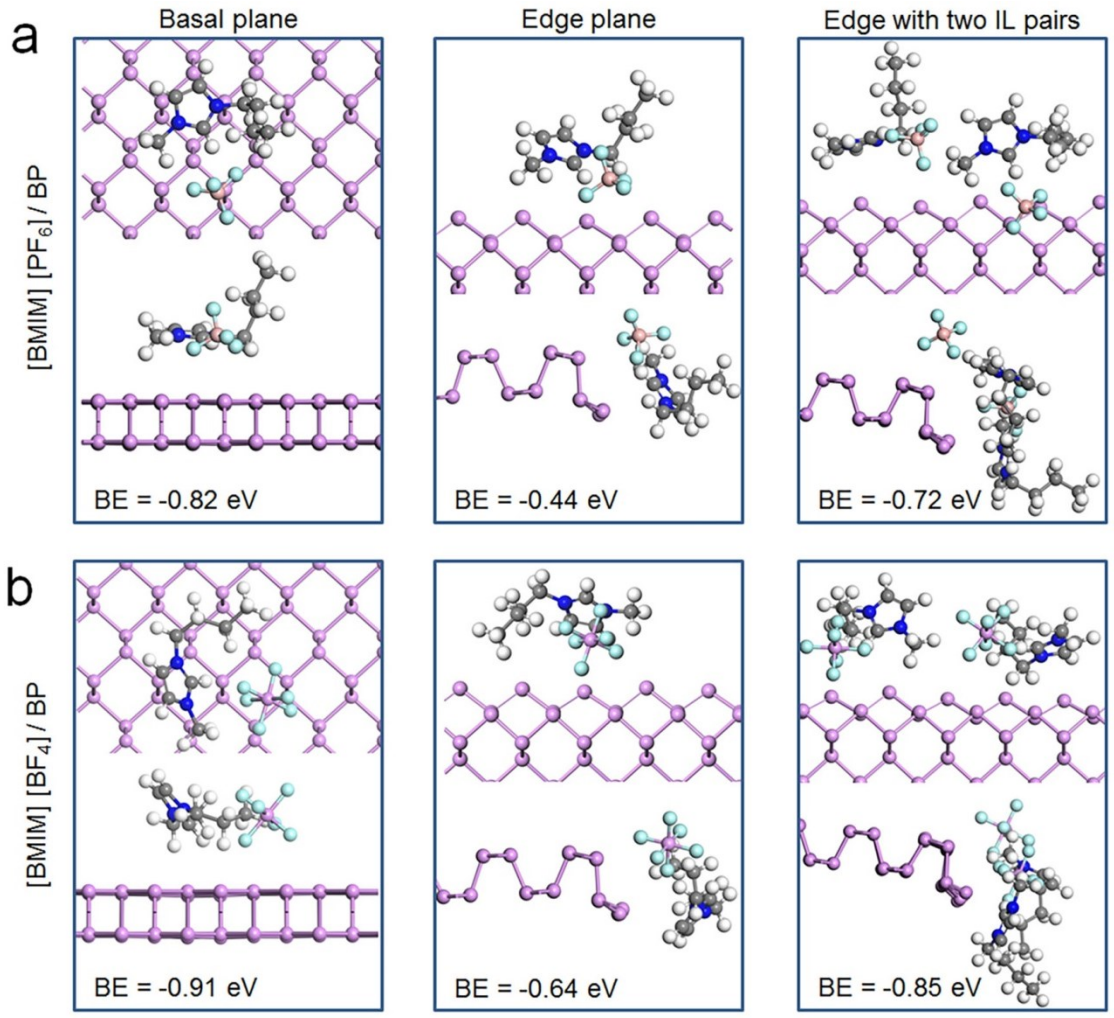

Figure 2. (Left to right) DFT-calculated thermodynamically favoured structures and corresponding binding energies for ILs. a) [BMIM][PF_6] and b) [BMIM][BF_4] chemisorption on BP basal plane, edge plane and with two IL pairs on the edge plane. It is evident that the [BMIM][BF_4] binds more strongly to both BP planes compared to [BMIM][PF_6].

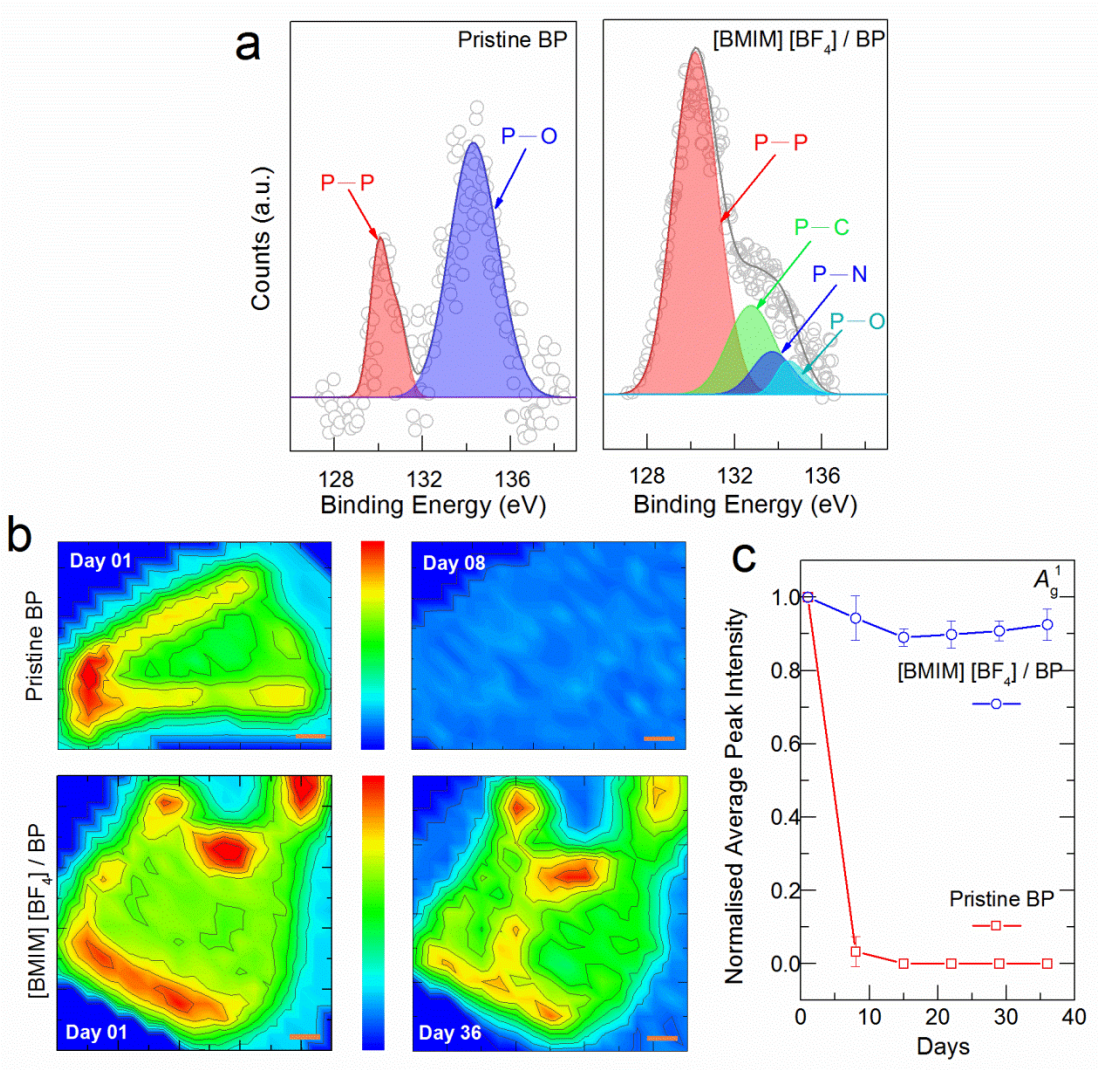

Figure 3. a) Deconvoluted P 2*p* core-level XPS spectra after 72 h of ambient exposure for a pristine and a [BMIM][BF_4]-treated BP flake. The evolution of the P–O feature at 134.1 eV in pristine BP is indicative of the photo-oxidation at the surface within 72 hours. In the case of a surface-treated BP flake, the P–P, P–C and P–N features are predominant. b) Spatial Raman peak intensity maps (A^1_g) for a representative pristine BP flake (Day 01 and 08) and [BMIM][BF_4]-treated BP flake (Day 01 and 36). Scale bars denote 1 µm. Corresponding pixel-by-pixel map is shown in Supporting Figure S10. c) Evolution of the normalised intensity (averaged from multiple BP flakes) of the A^1_g Raman mode over the course of ambient exposure. It can be seen that even after multiple exposures to the Raman laser, the

surface-treated flakes are largely preserved. The error bars represent a confidence interval of 95%.

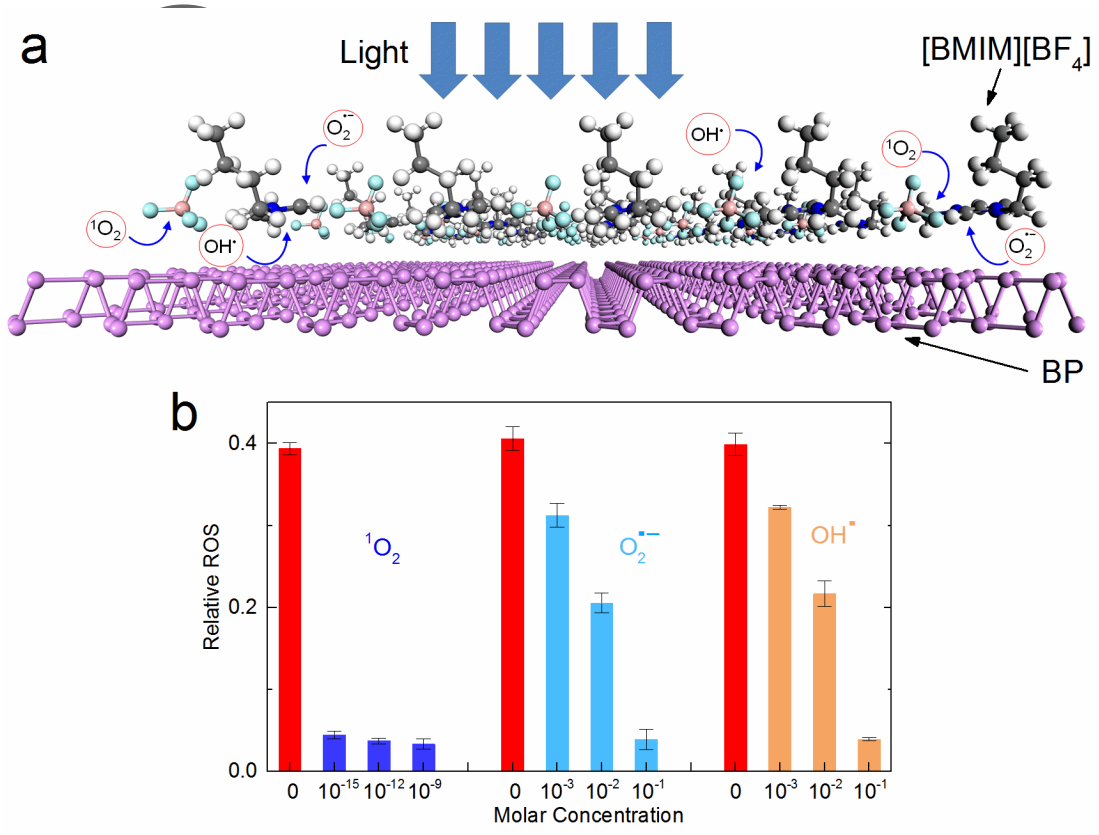

Figure 4. a) A schematic representation of the [BMIM][BF_4] IL-induced ROS sequestration mechanism on the BP surface. b) The ability of [BMIM][BF_4] to quench different photo-oxidative species, wherein the differences in the molar concentrations of the IL required to quench $^1O_2$, OH· and $O_2^{\bullet-}$ levels are notable.

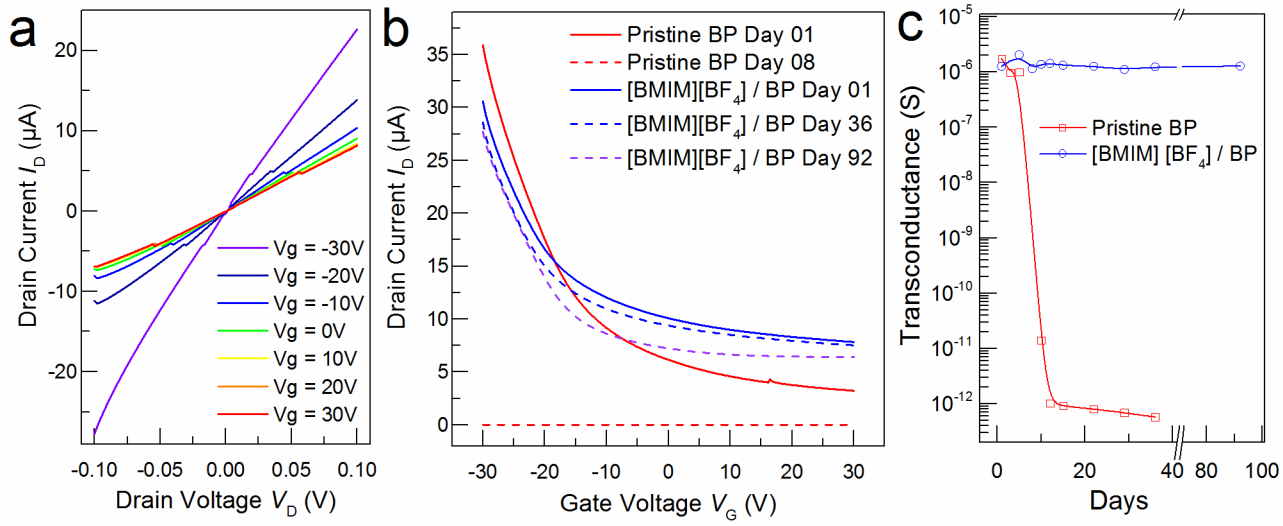

Figure 5. a) I_D–V_D curves of a [BMIM][BF_4]-treated BP FET with varying gate voltages. b) Transfer characteristics of a pristine and [BMIM][BF_4]-treated BP FET over the course of ambient exposure. c) comparison of transconductance of a pristine and [BMIM][BF_4]-treated BP FET over 92 days. It is seen that the characteristics of surface-treated BP FETs are preserved, whereas the electronic properties of the pristine BP FET shows rapid degradation within 8 days.

TOC entry

Few-layer black phosphorous (BP) has recently emerged as a promising candidate for next generation nanophotonic and nanoelectronic devices. However, rapid ambient degradation of mechanically-exfoliated BP poses challenges in its practical deployment in scalable devices. Here, we report an approach that allows this sensitive material to remain stable without requiring its isolation from the ambient environment. This chemical sequestration strategy allows BP to remain stable for over thirteen weeks, while retaining its key electronic characteristics. This study opens opportunities to practically implement BP and other environmentally-sensitive two-dimensional (2D) materials for electronic applications.

Keywords: phosphorene, black phosphorus, two-dimensional materials, stability, ionic liquids, degradation

Sumeet Walia*, Sivacarendran Balendhran, Taimur Ahmed, Mandeep Singh, Christopher El-Badawi, Mathew D. Brennan, Pabudi Weerathunge, Md. Nurul Karim, Fahmida Rahman, Andrea Rassell, Jonathan Duckworth, Rajesh Ramanathan, Gavin E. Collis, Charlene J. Lobo, Milos Toth, Jimmy Christopher Kotsakidis, Bent Weber, Michael Fuhrer, Jose Manuel Dominguez-Vera, Michelle J. S. Spencer, Igor Aharonovich, Sharath Sriram, Madhu Bhaskaran and Vipul Bansal*

Ambient protection of few-layer black phosphorus via sequestration of reactive oxygen species